Annales Geophysicae (2003) 21: 1073–1081

Annales Geophysicae

Verification of the backward wave oscillator model of VLF chorus generation using data from MAGION 5 satellite

E. E. Titova[1], B. V. Kozelov[1], F. Jiříček[2], J. Smilauer[2], A. G. Demekhov[3], and V. Yu. Trakhtengerts[3]

[1]Polar Geophysical Institute, Apatity, Russia
[2]Institute of Atmospheric Physics, Prague, Czech Republic
[3]Institute of Applied Physics, Nizhny Novgorod, Russia

Received: 12 April 2002 – Revised: 24 October 2002 – Accepted: 13 November 2002

Abstract. We present a detailed study of chorus emissions in the magnetosphere detected on board Magion 5, when the satellite was not far from the magnetic equator. We determine the frequency sweep rate of more than 8500 electromagnetic VLF chorus elements. These results are compared with the backward wave oscillator (BWO) regime of chorus generation. Comparison of the frequency sweep rate with the BWO model shows: (i) There is a correlation between the frequency sweep rates and the chorus amplitudes. The frequency sweep rate increases with chorus amplitude, in accordance with expectations from the BWO model; (ii) The chorus growth rate, estimated from the frequency sweep rate, is in accord with that inferred from the BWO generation mechanism; (iii) The BWO regime of chorus generation ensures the observed decrease in the frequency sweep rate of the chorus elements with increasing L-shell.

Key words. Magnetospheric physics (VLF emissions, energetic particles) – Space plasma physics (wave-particle interactions)

1 Introduction

Generation of chorus emissions is one of the most puzzling problems of VLF waves in the Earth's magnetosphere. These emissions are the most intense of all natural VLF waves in the frequency range from a few hundred Hz to several kHz. They are observed as a succession of repeating discrete elements with rising frequency. It is generally accepted that the chorus is generated in a near-equatorial region by the cyclotron instability of radiation belt electrons. The cyclotron interaction of VLF waves and energetic particles can explain many of the chorus features, such as the relation of chorus frequency to the equatorial electron gyrofrequency, the maximum of chorus intensity in the equatorial cross section of the magnetic flux tube, and the relationship of chorus with precipitation of energetic (10–100 keV) electrons. Helliwell (1965, 1969) and Sazhin and Hayakawa (1992) reviewed these and other characteristics of chorus.

However, mechanisms responsible for the origin of chorus succession and formation of spectrum of separate chorus elements are both still not clear. Helliwell (1967) was the first to suggest the idea of how the frequency spectrum of discrete elements is formed. The phenomenological model by Helliwell (1967) is based on simultaneous fulfillment of the first- and second-order cyclotron resonance conditions of whistler wave interaction with energetic electrons. The model by Helliwell (1967) was repeatedly applied for interpretation of a spectrum of separate discrete elements, observed in the experiment. However, application of the Helliwell's model for chorus elements was not successful and Skoug et al. (1996) did not bring into accord the spectrum of chorus and the energy of the microburst electron precipitation detected simultaneously.

Further analytical and computational calculations (Nunn, 1974, Karpman, 1974) confirmed the idea of the second order cyclotron resonance and showed that discrete elements with varying frequency may be triggered by a quasi-monochromatic wave under the interaction with energetic electrons in the inhomogeneous magnetic field. The nonlinear theory of triggered emissions (Omura et al., 1991; Trakhtengerts et al., 2001) showed that the initial wave packet forms an electron beam, which then generates secondary waves of various spectral forms. The similarity between the spectra of chorus and triggered emissions indicates that chorus could be generated in the same way as triggered emissions. However, it was not clear how a succession of quasi-monochromatic signals and/or intense electron beams can appear in the region of chorus generation.

Recently, Trakhtengerts (1999) suggested a mechanism of chorus generation based on the backward wave oscillator (BWO) regime of magnetospheric cyclotron maser (Trakhtengerts, 1995). The BWO regime of chorus generation gives hope of explaining such features of chorus as the appearance of a succession of discrete elements and their spectrum, the

Correspondence to: E. E. Titova
(titova@pgi.kolasc.net.ru)

relationship of chorus to ELF hiss, the large growth rates of chorus, and the different generation regimes such as quasi-periodic and stochastic ones. The suggested BWO model of chorus generation allows for a number of predictions that can be checked experimentally. In this paper we compare spectral and amplitude characteristics of chorus observed on board the MAGION 5 satellite with those predicted by the backward wave oscillator model of chorus generation.

2 The BWO regime of chorus generation in the magnetosphere

In this section, we briefly review the BWO regime of whistler wave generation in the magnetosphere (Trakhtengerts 1995, 1999) to select the parameters that can be compared with experimental data. This regime is similar to the backward wave oscillator in laboratory electronic devices, where the wave propagates opposite to the motion of an interacting electron (Ginzburg and Kuznetsov, 1981). Similar wave-particle interactions take place in the magnetospheric cyclotron maser. The generation of chorus is based on the cyclotron resonance of radiation belt electrons with whistler waves

$$\omega - \omega_H = k_\parallel v_\parallel, \tag{1}$$

where ω is the wave frequency, ω_H is the electron gyrofrequency, $k_\parallel$ and $v_\parallel$ are the magnetic field-aligned components of the wave vector and electron velocity.

Certain conditions have to be satisfied for a generator to operate in the BWO regime. The first condition requires that the phase velocity component along the magnetic field should be opposite to the electron motion. According to (1), this condition is satisfied if $\omega < \omega_H$. The second condition is the existence of a well-organized electron beam with small velocity dispersion in the region of chorus generation. This condition poses a significant problem, since there is no obvious reason for such a beam to be formed. The solution of this problem can be related to the fact that cyclotron interaction of band-limited natural ELF/VLF noise-like emissions with energetic electrons results in the formation of a specific step-like feature of the distribution function, shown in Fig. 1a (Trakhtengerts et. al., 1986, 1996; Nunn and Sazhin, 1991). This step-like deformation of energetic electron distribution function ensures a large growth rate $\gamma_{\rm HD}$ of whistler waves and transition to the BWO regime, which leads to the generation of a succession of discrete signals with rising frequency inside each element. Trakhtengerts (1995) showed that the step-like deformation of the distribution function, caused by interactions of natural ELF/VLF noise-like emissions and energetic electrons, acts in the magnetosphere as a well-organized beam in laboratory devices. A schematic picture of wave and electron motion in the magnetospheric BWO is shown in Fig. 1b. The BWO generation regime develops within a narrow region near the equatorial plane, and a positive feedback is provided by the electron beam itself. In a laboratory BWO, the interaction length is the size of the device. The magnetospheric BWO has no fixed boundaries, and its interaction length l is determined by the inhomogeneity of the geomagnetic field. According to Helliwell (1967) and Trakhtengerts (1995), the interaction length l of whistler waves and energetic electrons can be written for the dipole magnetic field as follows:

$$l = (R_0^2 L^2/k)^{1/3}, \tag{2}$$

where R_0 is the Earth's radius, L is the geomagnetic shell, and k is the whistler wave number.

The BWO generation starts when the density of energetic electrons exceeds some threshold value. According to Trakhtengerts (1995), this threshold condition can be written as

$$p = 2\gamma_{\rm HD} l / \left[\pi (V_\parallel V_g)^{1/2}\right] = 1, \tag{3}$$

where l is the working length of the magnetospheric generator, V_g is the group velocity of the whistler waves, $\gamma_{\rm HD} \sim (0.1\Delta n_h/n_c)^{1/2}\omega_H$ is the hydrodynamic growth rate in the case of the distribution function with a step-like deformation, Δn_h is the height of a step, and n_c is the cold plasma density. The BWO (chorus generation) growth rate can be written as a function of p in the form (Trakhtengerts, 1999):

$$\gamma_{\rm BWO} = 2p(p-1)T^{-1}, \tag{4}$$

where

$$T = 1.6l\left(V_g^{-1} + V_\parallel^{-1}\right). \tag{5}$$

If the step height increases, the BWO generation regime changes from the stationary generation that takes place for $1 < p < p_2$ to the periodic one with the period T for $p_2 < p < p_3$. Further increase in the parameter $p > p_3$ leads to the stochastic generation regime with random variation of the wave amplitude in time. The bifurcation values $p_{2,3}$ are equal to: $p_2 = 2$, and $p_3 = 4.5$ for laboratory devices (Ginzburg and Kuznetsov, 1981). To obtain the bifurcation values $p_{2,3}$ for chorus, it is necessary to develop the strict nonlinear theory for the magnetospheric BWO, which is absent now. Therefore, taking into account a big similarity in laboratory and magnetospheric BWO generators, we will take for further estimations the laboratory values of $p_{2,3}$. Dynamic spectra of VLF emissions, corresponding to different regimes of the magnetospheric BWO generator, are schematically represented in Fig. 1c.

After transition to the periodic BWO regime ($p_2 > 2$), the dynamic spectrum of a separate chorus element is formed similar to discrete signals triggered by VLF transmitters (Nunn, 1974; Omura et al., 1991; Trakhtengerts et al., 2001). In this case, the frequency sweep rate df/dt ($f \equiv \omega/2\pi$) at the exit from the BWO generation region can be written as

$$df/dt = \left[\Omega_{\rm tr}^2 + 3V_\parallel (d\omega_H/dz)\right] \cdot 0.15\omega/(\omega_H + 2\omega), \tag{6}$$

where the trapping frequency Ω_{tr} is determined by the expression

$$\Omega_{\rm tr} = (ku\omega_H b)^{1/2}. \tag{7}$$

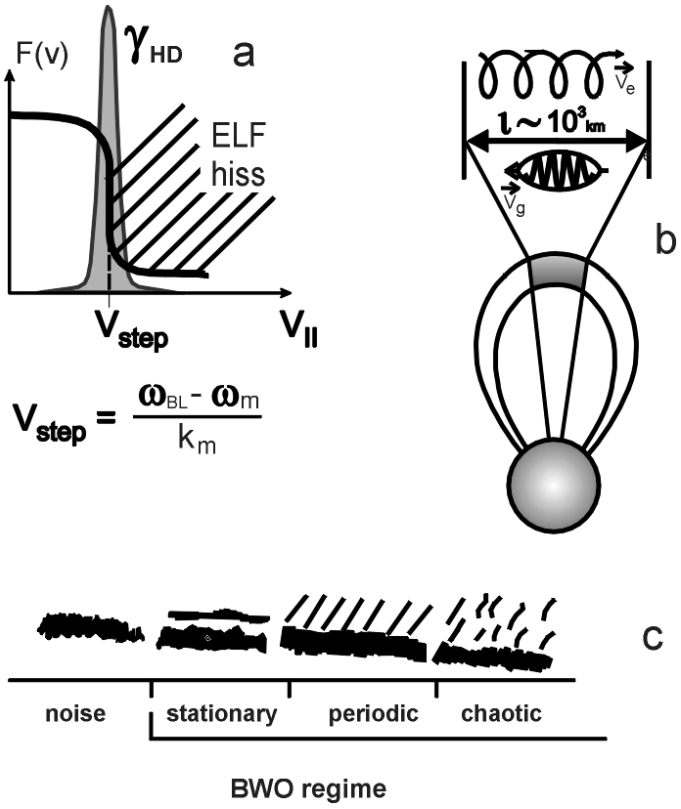

Fig. 1. (a) A schematic picture of a specific step-like deformation of the distribution function by cyclotron interactions of a natural ELF/VLF noise-like emissions and energetic electrons. This step-like deformation of energetic electron distribution function ensures the large growth rate of the whistler waves and transition to the BWO generation regime, which forms a succession of discrete signals. **(b)** Schematic picture of the BWO generation regime for chorus generation in the magnetosphere. **(c)** Dynamic spectra of VLF emissions, corresponding to different regimes of the magnetospheric BWO generator.

Here, $b = B_{\sim}/B_L$, $B_{\sim}$ is the whistler wave magnetic field amplitude, B_L is the geomagnetic field, and u is the electron velocity component across the geomagnetic field. There is the additional relation between the chorus amplitude and the BWO growth rate (Trakhtengerts, 1999):

$$\gamma_{\mathrm{BWO}}/\,\Omega_{\mathrm{tr}} \approx 3\pi/32, \tag{8}$$

where γ_{BWO} is determined by Eq. (4). Taking Eq. (8) into account, we can rewrite Eq. (6) in the form

$$df/dt = (\gamma^2_{\mathrm{BWO}} + S_1)1.5\omega/(\omega_H + 2\omega), \tag{9}$$

where $S_1 = 0.3V_{\|}(d\omega_H/dz)$ characterizes the magnetic field inhomogeneity effect. One can see from Eq. (9) that, if $S_1 \ll \gamma^2_{\mathrm{BWO}}$, chorus elements are formed mainly inside the BWO generator, and the corresponding frequency variation is determined by nonlinear effects. In the opposite case, the frequency shift is determined by the magnetic field inhomogeneity factor S_1.

Since the frequencies (ω/ω_H) of the observed chorus elements are spread rather widely (see below), it is convenient to group the experimentally known values in Eq. (9) in a new function

$$G^2 \equiv df/dt(\omega_H + 2\omega)/1.5\omega = \gamma^2_{\mathrm{BWO}} + S_1 \tag{10}$$

which we call thereafter the "reduced" frequency sweep rate. Note that G is equal to the BWO growth rate if the frequency shift is determined by nonlinear processes ($\gamma^2_{\mathrm{BWO}} \gg S_1$). As one can see from Eqs. (6) and (7), the BWO model predicts an increase in frequency sweep rate df/dt and G^2 with chorus amplitude. These relationships are analyzed experimentally below on the basis of Magion 5 data.

3 Overview of data and the analysis procedure

We use new VLF broad-band measurements carried out on board the Magion 5 satellite for analysis of VLF chorus emissions detected not too far from the magnetic equator, i.e. from the generation region. Magion 5 was launched as a part of the INTERBALL mission at a highly elliptic orbit (Triska et al., 1996). The VLF broad-band measurements ($f < 22.5$ kHz) included both electric and magnetic field components.

Sample dynamic spectra of various types of magnetosphere chorus are demonstrated in Fig. 2. The upper panel shows discrete elements with almost constant frequency, that were observed at the upper boundary of the ELF hiss at orbit 4156 on 28 May 1999. Allcock and Mountjoy (1970)

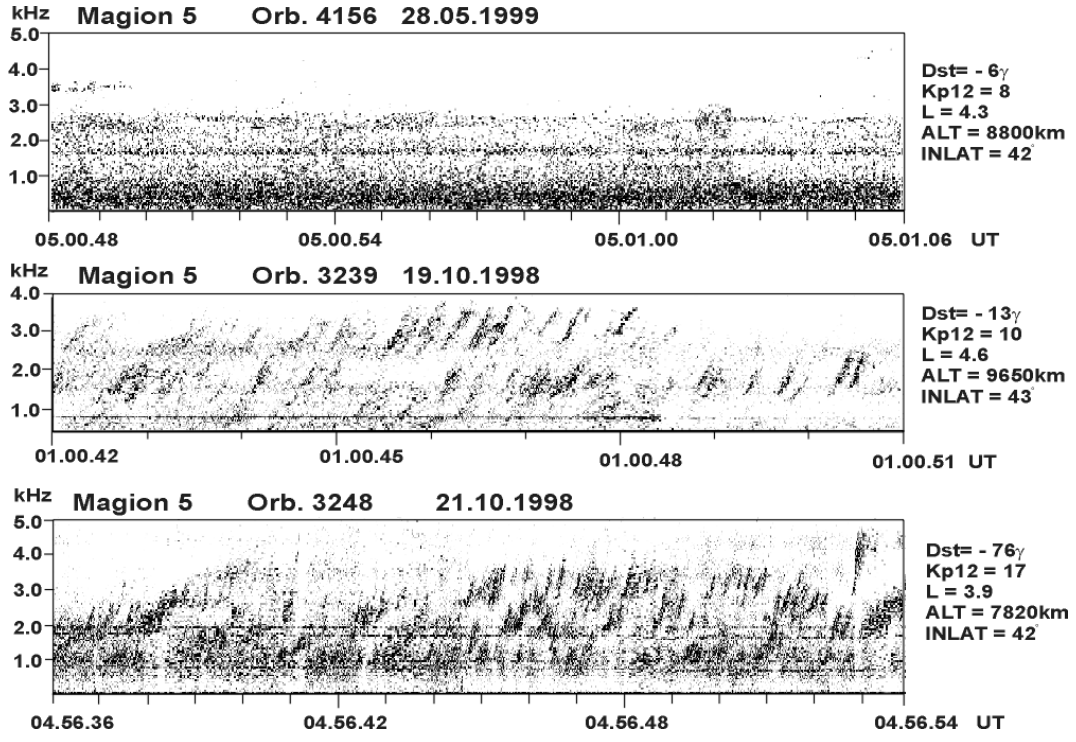

Fig. 2. Typical dynamic spectra of VLF chorus emissions on board of Magion 5 satellite for different magnetic disturbances. K_{p12} is the total value of K_p index for the preceding 12 h.

selected similar emissions as a special type of chorus (Q-chorus), observed on the ground during low magnetic activity. We should note that during orbit 4156 the magnetic activity was also very low ($D_{st} = -6\gamma$), and the total K_p index for the preceding 12 h was $\sum K_{p\,12} = 8$. The middle panel shows an example of quasi-periodic chorus. From the sonogram at orbit 3239 one can see that chorus is observed within two bands at frequencies below and above 3 kHz; the chorus group with a quasi-period of about 0.3 s is well seen at frequencies of 3–5 kHz. The lower panel shows a typical example of "chaotic" chorus, usually observed for a greater magnetic disturbance. In such a case, chorus elements appear irregularly at different frequencies, and it is impossible to define either the repetition quasi-period of discrete elements or the frequency band of chorus. One can see that spectra of chorus detected by Magion 5 are similar to the schematic wave spectra in Fig. 1c, corresponding to various regimes of BWO generation.

To obtain the frequency sweep rate df/dt, we have analyzed spectrum of chorus detected by the magnetic antenna along 10 orbits of Magion 5 in the morning sector (MLT<08) during the period from October 1998 to January 1999. The analysis was carried out for more than 8500 chorus elements, which were identified on sonograms. During that period Magion 5 was crossing the region of chorus registration at latitudes of 30°–40°. The VLF chorus was detected in the plasmapause region at L within 2.5 to 6. We have obtained the center frequency and the mean frequency sweep rate df/dt of each chorus element. The center frequency of an element was defined as $f_{\rm av} = (f_{\rm u} + f_{\rm l})/2$, where $f_{\rm u}$ and $f_{\rm l}$ are the maximum and minimum frequencies of the element, respectively. Note that for most chorus elements analyzed, the frequency sweep rate df/dt had an almost constant value within the entire frequency range of the element. Therefore, we were able to obtain df/dt by dividing the frequency spread $\Delta f = f_{\rm u} - f_{\rm l}$ of an element by its duration Δt.

The dependence of the center frequency f_{av} of the chorus elements on L-shell is shown in Fig. 3a. The frequencies of chorus were found within the frequency range 1–12 kHz, mainly (in 90% cases) within the band below 6 kHz. Figure 3a shows that the mean chorus frequency decreases with L as $L^{-2.5}$ (thin grey line). The thick grey line marks $f_H/4$, where f_H is the electron gyrofrequency at the equator. The analysis of the normalized frequency $f_{\rm av}/f_H$ of chorus elements shows that the mean $f_{\rm av}/f_H$ depends rather weakly on L-shell, varying from 0.2 to 0.25. However, the deviation from this mean value can be quite high (from 0.1 to 0.6). The frequency sweep rate df/dt of chorus elements as a function of L-shell is shown in Fig. 3b, where the mean rate decreases with L-shell as L^{-2} (grey line). It is noteworthy that the frequency sweep rates lie within the range from $10^3\,{\rm s}^{-2}$ to $10^5\,{\rm s}^{-2}$; in about 30% of all elements analyzed df/dt is higher than $10^4\,{\rm s}^{-2}$.

As it follows from Eq. (10), the quantity G^2, that we named the reduced df/dt, is more appropriate for comparison of observations with the BWO model, since, at first, it is directly related to the BWO growth rate and, secondly, it

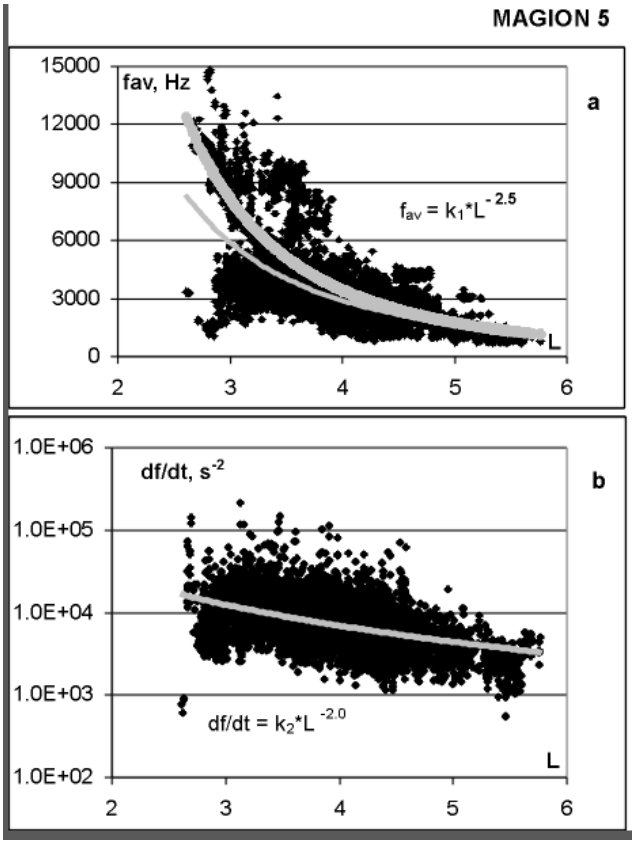

Fig. 3. (a) The center frequency of the chorus elements $f_{\rm av}$ depending on L-shell. Thick grey line marks $f_H/4$, where f_H is the electron gyrofrequency at the equator. The center frequency of the chorus band decreases with increasing L as $L^{-2.5}$ (thin grey line). **(b)** The frequency sweep rate of the chorus emissions depending on L-shell. The rate is rather high (higher than 10 kHz/s) for about 30% of all elements analyzed. The mean sweep rate decreases with L-shell as L^{-2} (grey line).

does not include the term depending on the highly variable ratio of f/f_H. To estimate the value of G^2, we need the frequency sweep rate df/dt and the average frequency $f_{\rm av}$ of chorus elements, both determined from Magion 5 data, and the equatorial electron gyrofrequency f_H on the same magnetic field line. To compute f_H, the dipole approximation for the geomagnetic field was applied, since electromagnetic chorus at frequencies $f < f_H/2$ near the equator propagate at a small angle to the geomagnetic field line (e.g. Goldstein and Tsurutani, 1984) and, therefore, we assumed that they were generated and detected at the same L-shell.

4 Results of observations and their comparison with the BWO model

4.1 Relation between the frequency sweep rate and chorus amplitude

According to the BWO model, the frequency sweep rate in a chorus element is a function of the characteristic chorus amplitude. Unfortunately, we had some technical problems with the measurements of absolute amplitude for the chorus detected by Magion 5, so we analyzed variations of the relative amplitude of chorus. We determined the average value of amplitude in each chorus element for 7 orbits of Magion 5.

From those orbits we selected two with the largest df/dt (orbits 3240 and 3322) and two with the smallest df/dt (orbits 3248 and 3239). Figures 4a and b show df/dt chorus elements and Figs. 4c and d show relative chorus amplitudes for those orbits as functions of L-shell. The comparison between Figs. 4a and b demonstrates that df/dt detected at orbits 3240 and 3322 are, indeed, distinctly larger than at orbits 3248 and 3239. From Fig. 4 we can also see that at the same L-shells, the amplitudes of chorus with larger df/dt definitely exceed those with smaller df/dt. The reduced frequency sweep rate G^2, in which the effects of spread in f/f_H are eliminated, also increases with the amplitude (Figs. 4e and f). Such a dependence is in agreement with predictions of the BWO model for chorus generation (see Eqs. 7–10).

The importance of using the reduced frequency sweep rate G^2 instead of df/dt is demonstrated by the sample data detected on orbit 3330 of Magion 5 and shown in Fig. 5. The top panel shows the frequency sweep rate df/dt and the center frequency of the chorus elements $f_{\rm av}$, depending on L-shell. The bottom panel of Fig. 5 shows the chorus amplitudes along this orbit. Chorus emissions were detected at $L = 3.2 - 4.5$. The specific feature of this orbit is that the mean df/dt almost did not vary along the entire satellite pass, while both the frequency and amplitude of chorus varied considerably, with the frequency decreasing from $f_{\rm av} = 10$ kHz at L= 3.3 to $f_{\rm av} = 2$ kHz at $L = 3.8 - 4.5$ and the amplitude increasing approximately 4 times in the same range of L. Note that the change in both amplitude and frequency occurs near the density drop, which is seen from the data on the cold plasma density (bottom panel). Due to the fast variations in the frequency and amplitude, the direct correlation between df/dt and the amplitude is not seen in this case, but a good correlation exists between the amplitude and G^2 is evident from Fig. 5b, which is in accordance with the BWO model.

4.2 Absolute values of the reduced frequency sweep rates of chorus G^2 and their dependence on L-shell

Figure 6 shows the L dependence of the reduced frequency shift G^2 (10). The solid line shows the running average over 100 points of G^2. It is seen that G^2 decreases in both directions from the maximum reached about $L = 3.2$. The decrease at smaller L can be related to the fact that these points correspond to the inner plasmasphere region, where the chorus amplitude is known to decrease inwards. At $L >$3.2, G^2 decreases as L^{-3}.

Now we compare the experimentally obtained values of G and their dependence on L with estimations based on the BWO model. According to Eq. (10), two terms give the additive contribution to the value of G, the first one is the nonlinear term, which can be expressed in terms of the BWO

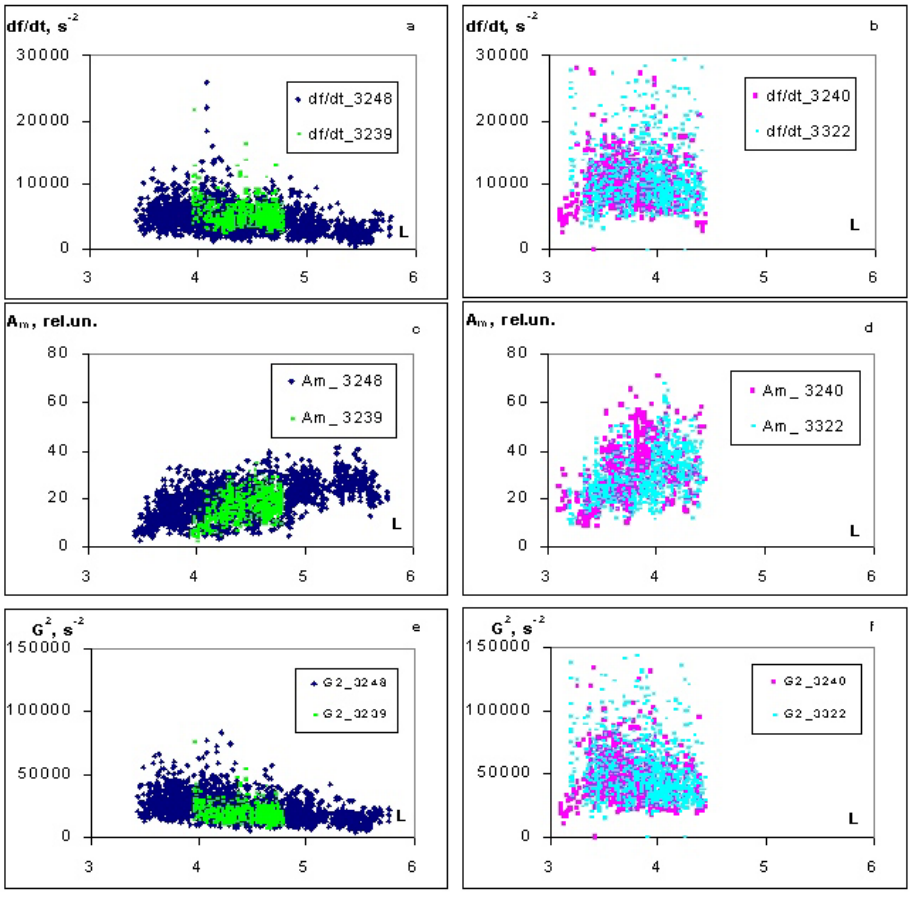

Fig. 4. The frequency sweep rate df/dt **(a, b)**, chorus amplitudes **(c, d)**, and G^2 **(e, f)** as a function of L-shell for 4 orbits of Magion 5 satellite. Note that df/dt is significantly greater on orbits 3240 and 3322 than on orbits 3248 and 3239. Figure shows that the high frequency sweep rate df/dt and G^2 are observed on the orbits having high chorus amplitudes (orbits 3240, 3322).

growth rate $\gamma_{\rm BWO}$, and the second one is the linear term S_1 related to the magnetic field inhomogeneity.

According to Eqs. (6), (7), and (9),

$$S_1 = V_\parallel/3(d\omega_H/dz) = 1.5(V_\parallel/l)^2(1 - f/f_H)^{-1}. \quad (11)$$

Taking into account Eqs. (4) and (11), expression (10) can be rewritten as

$$G^2 = \gamma_{\rm BWO}^2 + S_1 = \gamma_{\rm BWO}^2 \left\{1 + 1.2(1 + f_H/2f)^2(1 - f/f_H)^{-1}/[p^2(p-1)^2]\right\}. \quad (12)$$

It is seen from Eq. (12) that the relation between S_1 and $\gamma_{\rm BWO}^2$ depends on f/f_H and p. For Magion 5 chorus, $f/f_H \approx 0.25$ is the typical value. Furthermore, we suggest that most chorus emissions in Magion 5 data are related to the periodic and stochastic regimes of BWO generation. This suggestion is supported by the types of chorus spectra. In this case, $\gamma_{\rm BWO}$ is determined by relation (4), where $p > 2$. Taking into account the relation $V_g/V_\parallel = 2f/f_H$, we obtain:

$$\gamma_{\rm BWO} = 2p(p-1)V_g/l(1 + 2f/f_H). \quad (13)$$

Using the typical group velocity of chorus $V_g = 2.5{\cdot}10^4\,{\rm km\,s^{-1}}$, $l = 10^3\,{\rm km}$, and $2f/f_H = 0.5$, we obtain $\gamma_{\rm BWO} = 70$–$200\,{\rm s^{-1}}$ for $p = 2$–3. Note that $S_1 \le \gamma_{\rm BWO}^2$ if $p \ge 2$, i.e. near the threshold of the periodic BWO regime. Therefore, $G \approx \gamma_{\rm BWO}$, and we can compare the above estimate for $\gamma_{\rm BWO}$ with the experimentally obtained values of G. According to Fig. 6, G lies between 100 and $300\,{\rm s^{-1}}$, which yields a good agreement between two independent estimates of $\gamma_{\rm BWO}$.

Taking into account these estimates and relations (7) and (8) and assuming that $ku \sim \omega_H$, the dependence of G^2 on L can be obtained in the form

$$G^2 \propto \Omega_{\rm tr}^2 \propto \omega_H B_\sim. \quad (14)$$

For the orbits where the relative wave amplitude was measured, we can plot the ratio of $G^2/B_\sim$ as a function of L. According to Eq. (14), this dependence should be the same as $\omega_H(L)$ i.e. $G^2/B_\sim \propto L^{-3}$. The value of $G^2/B_\sim$ depending on L-shell for 7 orbits of MAGION 5 is shown in Fig. 7. As is seen from Fig. 7, the value $G^2/B_\sim(L)$ indeed decreases as $L^{-2.9}$ (grey line). Therefore, the experiment again shows an agreement with the BWO model. Note that taking different orbits separately, we obtained slightly different indices ranging from 2.2 to 3.6 for the power-law fit of $G^2/B_\sim$.

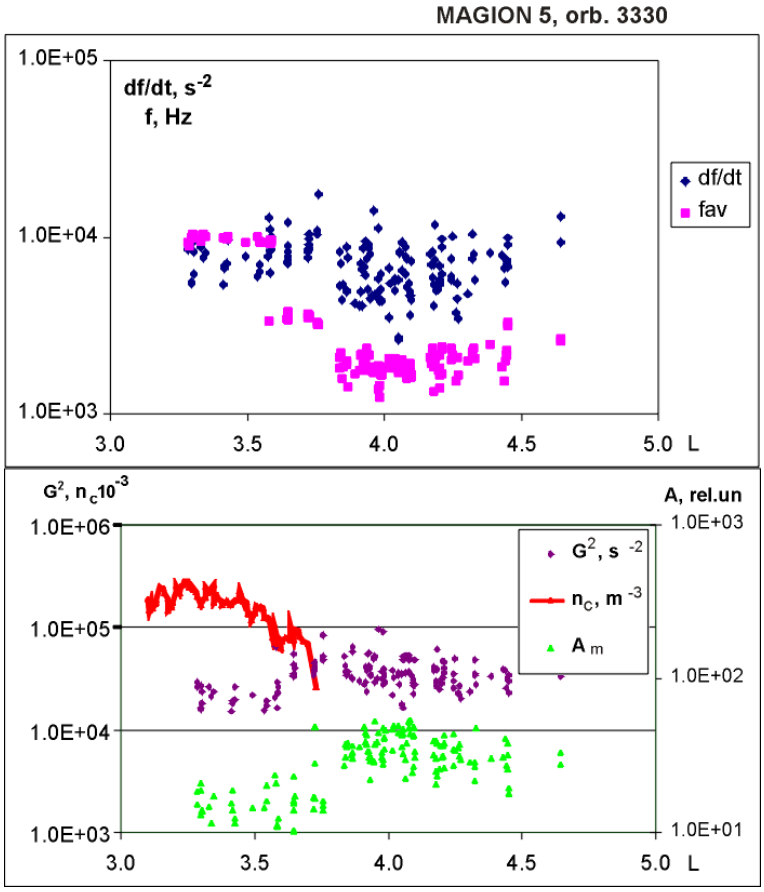

Fig. 5. Relationships of the frequency sweep rate df/dt and G^2 with chorus amplitudes on orbit 3330, MAGION-5. **Top panel:** The frequency sweep rate df/dt and the center frequency of the chorus elements f_{av} depending on L-shell for orbit 3330, Magion 5. **Bottom panel:** The chorus amplitude, G^2 and the cold plasma density n_c depending on L-shell for orbit 3330, Magion 5. Bottom panel shows a good correlation between G^2 and the chorus amplitudes in contrast to relationships between the frequency sweep rate df/dt and the chorus amplitudes.

Another possible test of the BWO model validity is based on the dependence of $\gamma_{\rm BWO}$ and G on the cold plasma density n_c. Indeed, it follows from Eqs. (12) and (13) that $G^2 \propto \gamma^2_{\rm BWO} \propto (V_g/l)^2 \propto n_c^{-2/3}$; therefore, strong variations in n_c should correlate with variations in G^2. Such a correlation is clearly seen in the Magion 5 data, e.g. on the lower panel in Fig. 5 showing the satellite motion towards higher latitudes. When the drop of density was crossed near $L = 3.5$, the cold plasma density n_c decreased more than an order of magnitude. At the same time, G^2 increased about 3–4 times, which corresponds to the BWO model both qualitatively and quantitatively.

5 Discussion and conclusions

Let us discuss the results obtained above in relation to previous studies of chorus spectral properties. Note that, although dynamical spectra of chorus have been studied in a multitude of papers, only several of them, written rather a long time ago, examined the frequency sweep rate of chorus.

Allcock and Mountjoy (1970) were the first to point out an increase in df/dt with increase in magnetic activity using ground-based observations of chorus. Sazhin and Titova (1977) confirmed that the values of df/dt increase with K_p and found these values to decrease with local time. Spectral characteristics of chorus elements observed on board equatorial satellites appeared to be essentially the same as those detected on the ground (Burtis and Helliwell, 1976). Our results for spectral characteristics of chorus detected by Magion 5 basically agree with those of Burtis and Helliwell, based on OGO 3 data. Some differences in the chorus characteristics are due to the fact that we analyze only the chorus observed in the early morning sector, while chorus properties, such as frequencies, inclinations, and latitudes of their registrations depend strongly on MLT. For instance, as the activity increases, chorus on the ground are observed during earlier hours and they have greater frequency sweep rates. This is why df/dt of chorus elements at Magion 5 exceed the values measured at OGO 3 approximately three times.

It is interesting to note that the existence of different generation regimes of chorus, following from the BWO theory,

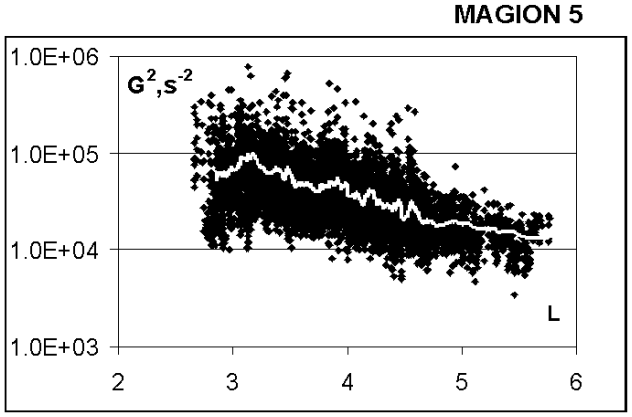

Fig. 6. The reduced sweep rate G^2 as a function of L-shell. The solid line shows the running average over 100 points of G^2. The mean $G(L)$ varies within a small interval 100–300 s^{-1}.

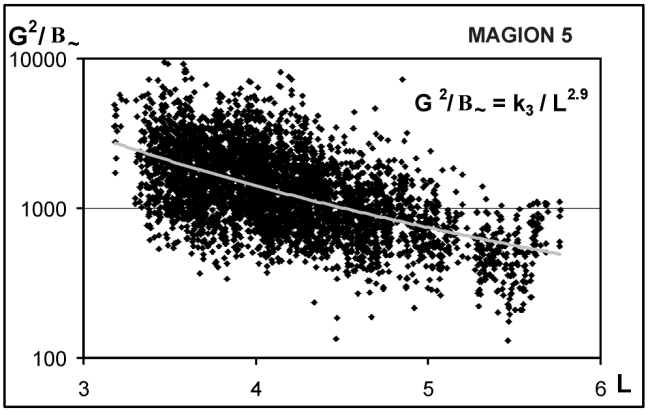

Fig. 7. The value of $G^2/B_\sim$ depending on L-shell for 7 orbits of MAGION 5. $B_\sim$ is the whistler-wave magnetic field amplitude. Note that $G^2/B_\sim(L)$ indeed decreases as $L^{-2.9}$ (grey line) in good agreement with BWO model.

is confirmed by the results of the earlier ground-based observations of chorus (Allcock and Mountjoy, 1970; Sazhin and Titova, 1977). Allcock and Mountjoy detected, as early as in 1970, the two main types of chorus spectrum, observed in quiet (a Q-type) and disturbed (an S-type) geomagnetic conditions. Existence of these types of chorus spectra can be related to different regimes of VLF wave generation in the magnetospheric BWO, i.e. to the stationary and chaotic regimes, respectively. In theory, the transition from the stationary to the chaotic regime is related to the increase in energetic electron density that certainly occurs with an increase in the magnetic disturbance level.

Using the chorus frequency drifts measured by Magion 5 and the BWO theory, we estimated the chorus growth rates to be about $10^2\,s^{-1}$. This is in agreement with both theoretical estimates (Trakhtengerts, 1999) and previous experimental results. In particular, Burtis and Helliwell (1975) found from the OGO 1 satellite data that the chorus amplitude was often growing exponentially in time with the growth rate ranging from 200 to 2000 dB s^{-1}, i.e. 45 to 450 s^{-1}. Note that, according to the BWO theory, the chorus generation region is very small, i.e. about 1000 km near the magnetic equator. This fact, confirmed by recent measurements on board Polar (LeDocq et al., 1998), can result in an overestimate of the growth rate based on indirect measurements, if one assumes the convective growth of chorus. For example, LeDocq et al. (1998) estimated the necessary convective growth rate to be at least $10^3\,s^{-1}$ using the typical group velocity of whistlers at about $2{\cdot}10^4$ km s^{-1}. However, such large values of the growth rate are not required if one takes into account the transition to the absolute instability, i.e. to the BWO regime of chorus generation.

Comparison of chorus frequency sweep rate with their amplitudes was performed earlier by Burtis and Helliwell (1975) using the data from OGO 1 and 3. They did not find a definite correlation between the chorus sweep rates and amplitudes. This conclusion differs from our results, which can be explained as follows. First, as is seen from Magion 5 data, it is not df/dt itself but the reduced inclination G^2 that correlates better with chorus amplitudes. Second, the relation between the chorus frequency sweep rates and amplitudes can be revealed only by using a much larger data volume than was reported by Burtis and Helliwell (1975). In typical situations, Magion 5 data taken along a single orbit also do not show a clear correlation between df/dt and the amplitude due to the large spread in parameters. Note, however, that the value of G^2 does correlate with chorus amplitude even along a single satellite orbit (see Fig. 5).

Let us estimate amplitudes of whistler waves following from the BWO theory. Using Eqs. (7) and (8) and substituting the typical frequency $f/f_H \approx 0.25$ for Magion 5 chorus, we can estimate the chorus amplitude corresponding to the BWO model as $B_\sim \approx 6 \cdot G^2/f_H$. It can be deduced from Fig. 6 that the value of G^2/f_H in the experiment varied within the range G^2/f_H=1–6 s^{-1}. Therefore, the amplitude in the BWO should be $B_\sim \approx$ 6–36 pT. As noted above, we do not have absolute measurements of amplitude for Magion 5 data. However, these estimated values seem quite realistic according to previous studies. Such larger amplitudes are often detected by satellites. For example, Burtis and Helliwell (1975) report observations of 1 to 100 pT VLF chorus in the frequency range from 2 to 10 kHz on board OGO 1 and OGO 3. For ELF chorus below 1 kHz even the amplitudes far exceeding 100 pT were detected (Nagano et al., 1996). The largest reported chorus amplitudes we are aware of (1040 pT) were detected by GEOS 2 (Parrot and Caye, 1994). Large amplitudes (>0.5 mV/m) of ELF/VLF chorus were measured near the equator on board CRRES beyond the plasmapause at $3< L <7$ in the morning and day sectors during magnetic disturbances (Meredith et al., 2001).

The main conclusions of this study can be summarized as follows. We have analyzed the frequency sweep rates df/dt for more than 8500 chorus elements recorded by MAGION 5 satellite at latitudes of 30–40 degrees from the geomagnetic equator at $L = 2.5$–6 in the morning sector near the plasma-

pause. We have performed the first direct comparison of the scalings obtained experimentally with those following from the backward wave oscillator (BWO) theory for chorus generation. Observations showed both qualitative and quantitative agreement with the theory in the following tests:

1. There is a correlation between the frequency sweep rates and the chorus amplitudes. The frequency sweep rate increases with chorus amplitude, in accordance with expectations from the BWO model.

2. The chorus growth rate, estimated from the measured frequency sweep rate, is close to that calculated from the linear BWO theory and to that obtained in other studies.

3. The BWO regime of chorus generation explains the observed decrease in the frequency sweep rate of the chorus elements with increasing L-shell.

Unfortunately, the absence of absolute amplitude measurements on board Magion 5 does not allow us to perform a more detailed comparison of chorus properties with the BWO theory. Moreover, there is a large spread in chorus frequency drifts even at close frequencies and close latitudes along the same orbit. However, we think that the results presented in this paper show the great potential of the BWO scenario to explain main features of chorus generation. It seems that further efforts in experimental studies of chorus emissions should be directed towards using more detailed simultaneous high-resolution measurements of both energetic electrons and whistler waves.

Acknowledgements. This work was supported in part by INTAS (grant 99-0502) and Russian Foundation for Basic Research (grants No. 01-05-643829 and 02-02-17109), and partially by the grant A3042201 of GA CA. The first author thanks International Space Science Institute for the opportunity to work on this contribution.

Topical Editor G. Chanteur thanks two referees for their help in evaluating this paper.

References

Allcock, G. M. and Mountjoy, J. C.: Dynamic spectral characteristics of chorus at a middle-latitude station, J. Geophys. Res., 75 (13), 2503–2510, 1970.

Bespalov, P. A. and Trakhtengerts, V. Y.: The cyclotron instability in the Earth radiation belts, in: Reviews of Plasma Physics, (Ed) Leontovich, M. A., 10, 155–192, Plenum, New York, 1986.

Burtis, W. J. and Helliwell, R. A.: Magnetospheric chorus: occurrence patterns and normalized frequency, Planet. Space. Sci., 24, 1007–1023, 1976.

Burtis, W. J. and Helliwell, R. A.: Magnetospheric chorus: amplitude and growth rate, J. Geophys. Res., 80 (22), 3265–3270, 1975.

Ginzburg, N. S. and Kuznetsov, S. P.: Periodic and stochastic regimes in electron generators with distributed interaction, in Relativistic HF Electronics, Institute of Applied Physics, Gorky, USSR, 101–104, (in Russian), 1981.

Goldstein, B. E. and Tsurutani, B. T.: Wave normal directions of chorus near the equatorial source region, J. Geophys. Res., 89 (A5), 2789–2810, 1984.

Helliwell, R. A.: Low-frequency waves in the magnetosphere, Rev. Geophys., 7, 281–303, 1969.

Helliwell, R. A.: Whistlers and related ionospheric phenomena, Standford University Press, Palo Alto, Calif, 1965.

Helliwell, R. A.: A theory of discrete emissions from the magnetosphere, J. Geophys. Res., 72, 4773–4790, 1967.

Karpman V. I., Istomin, Y. N., and Shklyar, D. R.: Nonlinear frequency shift and self-modulation of the quasi-monochromatic whistlers in the inhomogeneous plasma (magnetosphere), Planet. Space Sci. 22(5), 859–871, 1974.

LeDocq, M. J., Gurnett, D. A., and Hospodarsky, G. B.: Chorus source locations from VLF Poynting flux measurements with the Polar spacecraft, Geophys. Res. Lett., 25 (21), 4063–4066, 1998.

Meredith, N. P., Horne, R. B., and Anderson, R. R.: Substorm dependence of chorus amplitudes: implications for the acceleration of electrons to relativistic energies, J. Geophys. Res., 106, 13 165–13 178, 2001.

Nagano, I. S., Yagitani, Kojima, H., and Matsumoto, H.: Analysis of wave normal and Poynting vectors of the chorus emissions observed by GEOTAIL, J. Geomagnetism and Geoelectricity, 48 (3), 299–307, 1996.

Nunn D.: A self-consistent theory of triggered VLF emission, Planet. Space Sci. 22, 349–378, 1974.

Nunn, D. and Sazhin, S. S.: On the generation mechanism of hiss-triggered chorus, Ann. Geophysicae, 9, 603–613, 1991.

Omura, Y., Nunn, D., Matsumoto, H., and Rycroft, M. J.: A review of observational, theoretical and numerical studies of VLF triggered emissions, J. Atmos. Terr. Phys., 53(5), 351–368, 1991.

Parrot, M. and Gaye, C. A.: A Statistical Survey of ELF Waves in a Geostationary Orbit, Geophys. Res. Lett., 21 (23), 2463–2466, 1994.

Sazhin, S. S. and Titova, E. E.: Dynamics of VLF chorus spectrum according to Lovozero station data, Cosmic Res., 16, 376–379, 1977.

Sazhin, S. S. and Hayakawa, M.: Magnetospheric chorus emissions: A review, Planetary and Space Science, 40 (5), 681–697, 1992.

Skoug, R. M., Datta, S., McCarthy, M. P., and Parks, G. K.: A cyclotron resonance model of VLF chorus emissions detected during electron microburst precipitation, J. Geophys. Res.,-Space Physics, 101 (A10), 21 481–21 491, 1996.

Trakhtengerts, V. Y.: Magnetosphere cyclotron maser: Backward wave oscillator generation regime, J. Geophys. Res., 100 (A9), 17 205–17 210, 1995.

Trakhtengerts, V. Y., Rycroft, M. J., and Demekhov, A. G.: Interrelation of noise-like and discrete ELF/VLF emissions generated by cyclotron interactions, J. Geophys. Res., 101, 13 293–13 303, 1996.

Trakhtengerts, V. Y.: A generation mechanism for chorus emission, Ann. Geophysicae, 17 (1), 95–100, 1999.

Trakhtengerts, V. Y., Hobara, Y., Demekhov, A. G., and Hayakawa, M.: A role of the second-order cyclotron resonance effect in a self-consistent approach to triggered VLF emissions, J. Geophys. Res., 106 (A3), 3897–3904, 2001.

Triska, P., Vojta, J., Base, J., Chum, J., Czapek, A., Hruska, F., Korab, J., Agafonov, Yu., Khrapchenkov, V., Friedrich, M., and Puerstl, F.: Small satellites for the INTERBALL mission, in: Small Satellites for Earth Observation, Proc. of the International Symposium of the IAA, (Eds) Roeser, H. P., Sandau, R., and Valenzuela, A., Berlin, 212–215, 1996.